

Electrochemical Performance and *ex situ* Analysis of ZnMn₂O₄ Nanowires as Anode Materials for Lithium Rechargeable Batteries

Sung-Wook Kim^{1,§}, Hyun-Wook Lee^{2,§}, Pandurangan Muralidharan^{2,§}, Dong-Hwa Seo², Won-Sub Yoon³, Do Kyung Kim² (✉), and Kisuk Kang^{2,4} (✉)

¹ Research Institute of Advanced Materials, Seoul National University, 599 Kwanak-ro, Kwanak-gu, Seoul 151-742, Republic of Korea

² Department of Materials Science and Engineering, Korea Advanced Institute of Science and Technology, 335 Gwahangno, Yuseong-gu, Daejeon 305-701, Republic of Korea

³ School of Advanced Materials Engineering, Kookmin University, 861-6 Jeongneung-dong, Seongbuk-gu, Seoul 136-702, Republic of Korea

⁴ Department of Materials Science and Engineering, Seoul National University, 599 Kwanak-ro, Kwanak-gu, Seoul 151-742, Republic of Korea

§ These authors contributed equally to this work

Received: 2 November 2010 / Revised: 10 January 2011 / Accepted: 12 January 2011

© Tsinghua University Press and Springer-Verlag Berlin Heidelberg 2011

ABSTRACT

One-dimensional ZnMn₂O₄ nanowires have been prepared and investigated as anode materials in Li rechargeable batteries. The highly crystalline ZnMn₂O₄ nanowires about 15 nm in width and 500 nm in length showed a high specific capacity of about 650 mAh·g⁻¹ at a current rate of 100 mA·g⁻¹ after 40 cycles. They also exhibited high power capability at elevated current rates, i.e., 450 and 350 mAh·g⁻¹ at current rates of 500 and 1000 mA·g⁻¹, respectively. Formation of Mn₃O₄ and ZnO phases was identified by *ex situ* X-ray diffraction (XRD) and transmission electron microscopy (TEM) studies after the initial discharge–charge cycle, which indicates that the ZnMn₂O₄ phase was converted to a nanocomposite of Mn₃O₄ and ZnO phases immediately after the electrochemical conversion reaction.

KEYWORDS

Energy storage, lithium rechargeable battery, anode, ZnMn₂O₄, nanowire

1. Introduction

Increasing demand for higher energy capability Li rechargeable batteries has led the extensive research efforts on the development of electrode materials with higher specific capacity [1–4]. In particular, materials that store Li ions through a conversion reaction (e.g., CoO, Co₃O₄, FeO, MnO₂) or an alloying reaction (e.g., Si, Ge, Sn) have been suggested as promising alternative anode materials due to their intrinsically high specific capacity [5–9]. However, these materials typically undergo significant volume

change during lithiation and delithiation due to the large Li uptake in the structure and accompanying phase transformation. In addition, electron (or Li-ion) conduction is often severely restricted during the electrochemical reaction. In this respect, fabrication of nanosized particles of these materials has been intensively explored and, in some cases, proven to effectively accommodate strain induced by volume change and give improved electron/Li-ion conduction [10–14].

Recent studies have shown that Si anodes exhibit promising electrochemical performance when properly

Address correspondence to Do Kyung Kim, dkkim@kaist.ac.kr; Kisuk Kang, matlgen1@snu.ac.kr



designed with nanosized particles [12–14]. However, fabrication of Si nanostructures frequently involves complex processes which require special chemical agents or apparatus, resulting in high production costs and restricting their potential for commercial development.

On the other hand, nanostructured transition metal oxides can be obtained even from simple basic processes such as solid-state, sol-gel, and hydrothermal synthesis methods [15–17]. Commercialization of these simple processes is therefore much more feasible. Nanostructured Co_3O_4 has been demonstrated as a promising anode material due to its high electrochemical activity and specific capacity ($\sim 900 \text{ mAh}\cdot\text{g}^{-1}$) [5, 11], although the high cost and toxicity of Co remain as major drawbacks.

Recently, compounds involving partial or total substitution of Co in Co_3O_4 , such as ZnCo_2O_4 , NiCo_2O_4 , and ZnMn_2O_4 have been proposed [18–21] as alternatives to Co_3O_4 . Of these, ZnMn_2O_4 is particularly interesting because all the Co ions have been substituted by cheap and non-toxic Zn and Mn ions [20, 21]. Interestingly, ZnMn_2O_4 can store Li ions through both conversion and alloying reactions because Zn, one of the products of the conversion reaction, further alloys with Li to form LiZn . Yang et al. and Xiao et al. investigated ZnMn_2O_4 nanoparticles and nanoflowers, which showed specific capacities as high as 569 and $626 \text{ mAh}\cdot\text{g}^{-1}$, respectively [20, 21].

In this study, we fabricate one-dimensional ZnMn_2O_4 nanowires by a simple synthesis process and demonstrate their use as a high performance anode material. *Ex situ* X-ray diffraction (XRD) and high resolution transmission electron microscopy (HRTEM) analysis of the nanowire single crystals has been used to investigate structural changes associated with the discharge-charge cycles.

2. Experimental

ZnMn_2O_4 nanowires were fabricated by a solid-state reaction of $\alpha\text{-MnO}_2$ nanowires and $\text{Zn}(\text{CH}_3\text{COO})_2$ (Aldrich, 99.99%). $\alpha\text{-MnO}_2$ nanowires were synthesized by hydrothermal reaction using $\text{Mn}(\text{CH}_3\text{COO})_2\cdot 4\text{H}_2\text{O}$ (Aldrich, 99.99%) and $(\text{NH}_4)_2\text{S}_2\text{O}_8$ (Aldrich 98%) [22]. A stoichiometric amount of the $\alpha\text{-MnO}_2$ nanowires

and $\text{Zn}(\text{CH}_3\text{COO})_2$ were homogeneously dispersed in high purity ethanol and diethylamine, and ground for several hours to form a fine mixture. Finally, the mixture was calcined at 480°C at low pressure in an O_2 atmosphere (2 mbar) for 12 h to form ZnMn_2O_4 nanowires.

The morphology of the ZnMn_2O_4 nanowires was confirmed by field emission scanning electron microscopy (SEM, Hitachi S-4800) and field emission TEM (JEOL JEM-2100F and Tecnai G² F30 S-Twin). The crystal phase of ZnMn_2O_4 was identified by XRD using $\text{Cu K}\alpha$ radiation (Rigaku D/MAX 2500). The electrochemical cells were assembled as CR2016-type coin cells composed of a ZnMn_2O_4 nanowire electrode, a Li metal counter electrode, a polymer membrane separator (Celgard 2400), and an organic electrolyte of 1 mol/L LiPF_6 in a 1:1 mixture of ethylene carbonate and dimethyl carbonate. A slurry composed of 60 wt.% ZnMn_2O_4 nanowire mixture, 30 wt.% carbon black, and 10 wt.% polyvinylidene fluoride binder was dissolved in *N*-methyl-2-pyrrolidone and manually mixed, cast onto Al foil, and then dried to form a test electrode. Electrochemical tests were performed using an automatic battery cycler (WonAtech, WBCS3000). Galvanostatic discharge-charge tests were performed in the voltage range 0.01–3.0 V at current rates from 100 to $1000 \text{ mA}\cdot\text{g}^{-1}$ and cyclic voltammetry (CV) was carried out in the same voltage range with a scan rate of $0.1 \text{ mV}\cdot\text{s}^{-1}$.

3. Results and discussion

The XRD pattern shown in Fig. 1(a) indicates that the fabricated powder is a conventional tetragonal ZnMn_2O_4 structure with the space group $I4_1/\text{amd}$ (JCPDS no. 24-1133). Figures 1(b)–1(d) show the typical morphology of the fabricated ZnMn_2O_4 nanowires which are about 15 nm wide and 500 nm long. Individual ZnMn_2O_4 nanowires are interwoven with each other to form a complex network structure. Compared with a simple spherical nanopowder, such a network structure is expected to improve the electrochemical performance, due to its higher resistance against separation or isolation of individual nanowires during the electrochemical reaction. This will be particularly critical for electrode materials experiencing

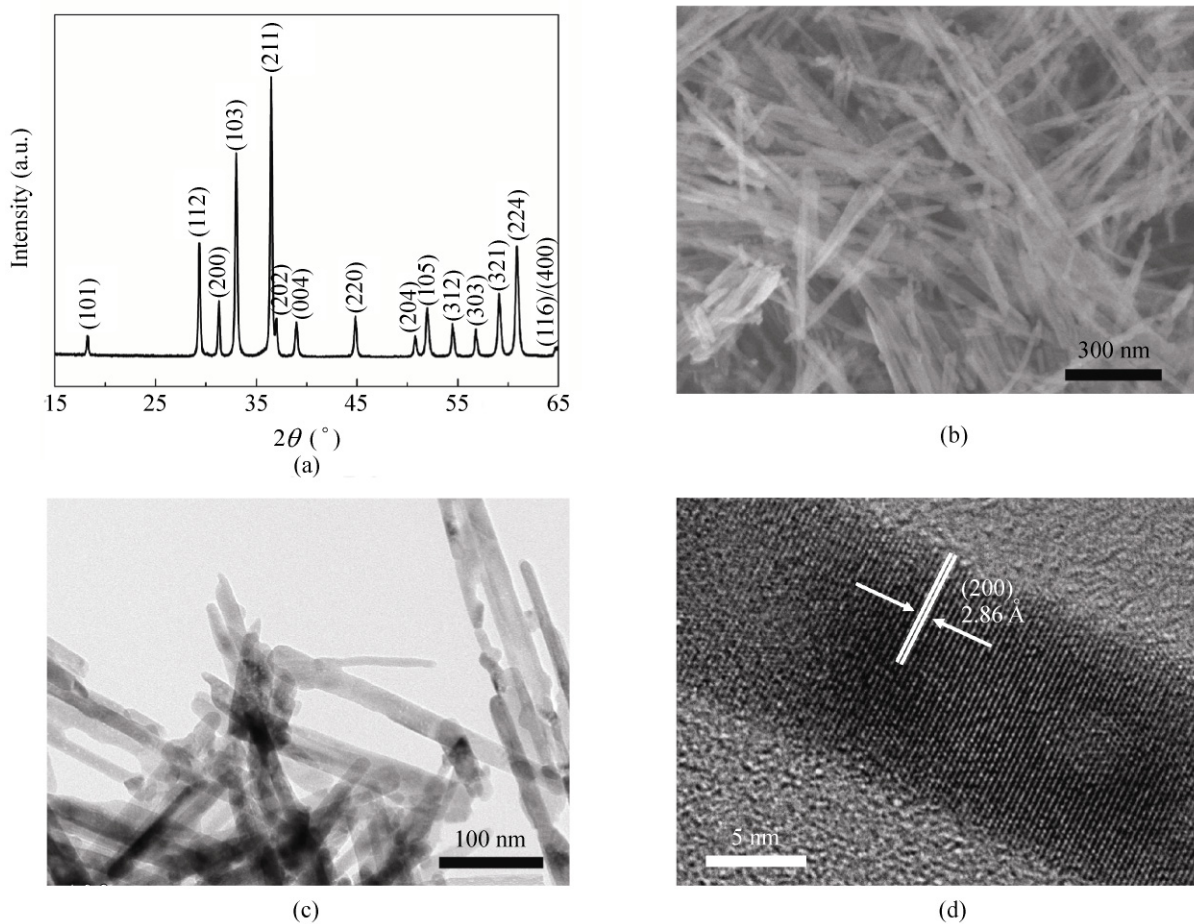


Figure 1 (a) XRD pattern and (b) SEM, (c) TEM, and (d) HRTEM images of the fabricated ZnMn_2O_4 nanowires

a large volume change. The HRTEM image shown in Fig. 1(d) indicates that the ZnMn_2O_4 nanowires are highly crystalline. The measured interplanar distance is about 2.86 Å which matches well to the (200) plane of ZnMn_2O_4 .

Electrochemical tests were performed using the ZnMn_2O_4 nanowire electrode as shown in Fig. 2. The galvanostatic discharge–charge profiles for the first five cycles at a current rate of $100 \text{ mA}\cdot\text{g}^{-1}$ are shown in Fig. 2(a). The first discharge capacity is about $1400 \text{ mAh}\cdot\text{g}^{-1}$ which is higher than the theoretical value ($1008 \text{ mAh}\cdot\text{g}^{-1}$). The formation of solid-electrolyte-interphase layers at the ZnMn_2O_4 /electrolyte interface may contribute to the extra capacity at the first discharge [20, 21]. The specific capacity is saturated at ca. $650 \text{ mAh}\cdot\text{g}^{-1}$ after several cycles, and this is comparable to that for ZnMn_2O_4 nanoflowers reported by Xiao et al. [21]. Figure 2(b) shows a comparison of

the specific capacity of ZnMn_2O_4 nanowires at different current rates. High rate performance of an electrode is especially important for high power applications, and the ZnMn_2O_4 nanowire exhibits good reversibility during the electrochemical reaction even at elevated current rates. The specific capacities were about 450 and $350 \text{ mAh}\cdot\text{g}^{-1}$ at a current rate of 500 and $1000 \text{ mA}\cdot\text{g}^{-1}$, respectively. This is the first report of such a high rate performance for a ZnMn_2O_4 anode material as far as we know. Considering that the highest power capability reported so far for ZnCo_2O_4 is about $350 \text{ mAh}\cdot\text{g}^{-1}$ at a current rate of $630 \text{ mA}\cdot\text{g}^{-1}$ [18] our ZnMn_2O_4 nanowire exhibits promising power capability.

Figure 2(c) shows the CV peaks of the ZnMn_2O_4 nanowire electrode. Compared to other ZnMn_2O_4 anodes with different morphologies [20, 21], the first irreversible reactions occurred at higher voltage near 1.6 and 1.3 V. It seems that the morphology of a

nanostructure influences the irreversible reaction voltage. After the irreversible reaction, the cathodic properties were comparable to those of other ZnMn_2O_4 anodes [20, 21]. On the other hand, the anodic peaks showed different behavior from these other ZnMn_2O_4 anodes. Xiao et al. suggested that the products after the first discharge— LiZn , Mn, and Li_2O —are converted to ZnO and MnO upon full delithiation [21]. They argued that anodic peaks near 1.2 and 1.5 V in a subsequent cycle are related to the conversion reactions of MnO and ZnO , respectively. However, one additional anodic peak near 2.2 V appeared for our material indicating that an additional oxidation step occurred during the delithiation.

In order to clarify the discharge–charge mechanism of ZnMn_2O_4 , we performed a structural investigation

using *ex situ* XRD and TEM. Figure 3(a) shows *ex situ* XRD patterns of the materials after the first discharge and charge, with that of pristine ZnMn_2O_4 for comparison. The crystalline ZnMn_2O_4 phase is completely destroyed after the initial discharge giving an amorphous-like phase, and is not recovered after the initial charge. This behavior is consistent with the Ref. [21]. Because it is hard to understand the reaction mechanism by XRD alone, we performed *ex situ* TEM analysis. In fact, it turns out that the use of single nanowires is beneficial for TEM structure analysis, since clear bulk images are readily obtained. Figure 3(b) shows the HRTEM images after initial discharge and charge. There are two crystalline domains clearly observed in the tested electrode. The interplanar distances in the two regions are about 2.49 Å and 2.82 Å, which

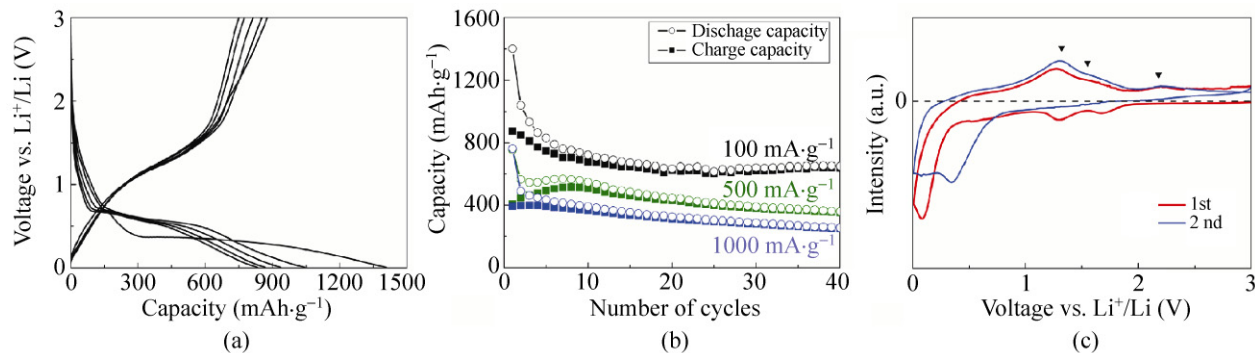


Figure 2 (a) Galvanostatic discharge–charge profiles of ZnMn_2O_4 nanowires for the first five cycles at a current rate of $100 \text{ mA}\cdot\text{g}^{-1}$. (b) Specific capacity of ZnMn_2O_4 nanowires over 40 cycles at different current rates. (c) CVs of ZnMn_2O_4 nanowires for the first two cycles at a scan rate of $0.1 \text{ mV}\cdot\text{s}^{-1}$

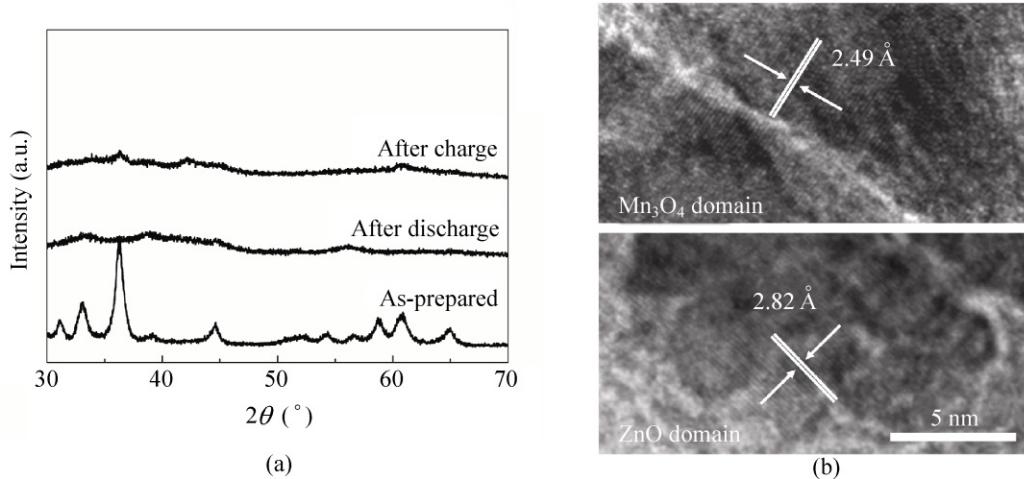
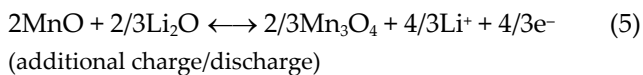
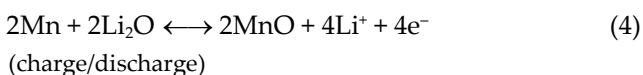
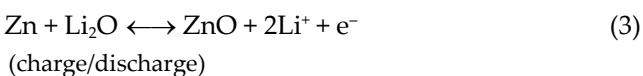
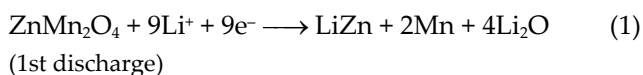


Figure 3 (a) *Ex situ* XRD patterns of ZnMn_2O_4 nanowires after the initial discharge–charge cycle. (b) Two crystalline domains of a ZnMn_2O_4 nanowire after the initial discharge–charge process, as observed by *ex situ* TEM

match to that of the (211) plane of the Mn_3O_4 phase (JCPDS no. 18-0803), and the (100) plane of the ZnO phase (JCPDS no. 36-1451), respectively. Considering that the oxidation reaction from CoO to Co_3O_4 occurs near 2.4 V during the charge process in a ZnCo_2O_4 anode [18], the additional CV peak observed near 2.2 V shown in Fig. 2(c) seems to be related to the oxidation of MnO to Mn_3O_4 , which is consistent with the *ex situ* TEM analysis. While Xiao et al. argued that the ZnMn_2O_4 phase converts to ZnO and MnO phases after electrochemical reaction [21], our results suggest that the ZnMn_2O_4 phase is transformed to ZnO and Mn_3O_4 . This discrepancy may be resolved by adding an additional oxidation step to the mechanism proposed by Xiao et al. during the charge process, as follows



We speculate that the additional electrochemical activity from MnO is possibly due to the enhanced kinetics of the nanowire electrode. More detailed studies to confirm this will be performed using *in situ* analysis in the near future.

4. Conclusion

ZnMn_2O_4 nanowires have been fabricated and electrochemically characterized as an anode material for Li rechargeable batteries. A ZnMn_2O_4 nanowire electrode can store and release Li^+ ions reversibly with a high specific capacity of ca. $650 \text{ mAh}\cdot\text{g}^{-1}$ at a current rate of $100 \text{ mA}\cdot\text{g}^{-1}$ and high power capability, with specific capacities of 450 and $350 \text{ mAh}\cdot\text{g}^{-1}$ at current rates of 500 and $1000 \text{ mA}\cdot\text{g}^{-1}$, respectively. From *ex situ* TEM

analysis of the nanowire electrode, we found that the ZnMn_2O_4 phase is converted to ZnO and Mn_3O_4 after the discharge–charge cycle. These ZnMn_2O_4 nanowires are expected to be a useful high performance anode material for future Li rechargeable battery applications.

Acknowledgements

This research was supported by the Energy Resource Technology Development program (No. 2008-E-EL11-P-08-3-010) and the Energy Resources Technology R&D program (No. 20092020100040) under the Ministry of Knowledge Economy. This research was also supported by the Nuclear R&D program (No. 2010-0018524), Engineering Research Center program (No. 2008-0062206) through the National Research Foundation (NRF) and Korea Science and Engineering Foundation (KOSEF) grant (No. R01-2008-000-20480-0) funded by the Ministry of Education, Science, and Technology (MEST). This research was also supported by the National Research Foundation of Korea Grant funded by the Korean Government (MEST) (NRF-2009-0094219). The *ex situ* TEM analysis was supported by “The Support Program for the Advancement of National Research Facilities and Equipment”, funded by the Korean government (MEST). P. M. was financially supported by the Priority Research Centers Program through the NRF funded by MEST (No. 2009-0094041). H. W. L. was supported by the NRF of Korea Grant funded by MEST (No. 2010-0029031).

References

- [1] Tarascon, J. M.; Armand, M. Issues and challenges facing rechargeable lithium batteries. *Nature* **2001**, *414*, 359–367.
- [2] Kang, K.; Meng, Y. S.; Bréger, J.; Grey, C. P.; Ceder, G. Electrodes with high power and high capacity for rechargeable lithium batteries. *Science* **2006**, *311*, 977–980.
- [3] Kim, D. K.; Muralidharan, P.; Lee, H. W.; Ruffo, R.; Chan, C. K.; Yang, Y.; Peng, H.; Huggins, R. A.; Cui, Y. Spinel LiMn_2O_4 nanorods as lithium ion battery cathodes. *Nano Lett.* **2008**, *8*, 3948–3952.
- [4] Kim, S. W.; Ryu, J.; Park, C. B.; Kang, K. Carbon nanotube-amorphous FePO_4 core–shell nanowires as cathode material for Li ion batteries. *Chem. Commun.* **2010**, *46*, 7409–7411.
- [5] Poizot, P.; Laruelle, S.; Gruegeon, S.; Dupont, L.; Tarascon,



- J. M. Nano-sized transition-metal oxides as negative-electrode materials for lithium-ion batteries. *Nature* **2000**, *407*, 469–499.
- [6] Lu, Y.; Wang, Y.; Zou, Y.; Jiao, Z.; Zhao, B.; He, Y.; Wu, M. Macroporous Co_3O_4 platelets with excellent rate capability as anodes for lithium ion batteries. *Electrochim. Commun.* **2010**, *12*, 101–105.
- [7] Ryu, J.; Kim, S. W.; Kang, K.; Park, C. B. Synthesis of diphenylalanine/cobalt oxide hybrid nanowires and their application to energy storage. *ACS Nano* **2010**, *4*, 159–164.
- [8] Fauteux, D.; Koksbang, R. Rechargeable lithium battery anodes: Alternative metallic lithium. *J. Appl. Electrochem.* **1993**, *23*, 1–10.
- [9] Wang, G. X.; Ahn, J. H.; Yao, J.; Bewlay, S.; Liu, H. K. Nanostructured Si–C composite anodes for lithium-ion batteries. *Electrochim. Commun.* **2004**, *6*, 689–692.
- [10] Bruce, P. G.; Scrosati, B.; Tarascon, J. M. Nanomaterials for rechargeable lithium batteries. *Angew. Chem. Int. Ed.* **2008**, *47*, 2930–2946.
- [11] Nam, K. T.; Kim, D. W.; Yoo, P. J.; Ching, C. Y.; Meethong, N.; Hammond, P. T.; Chiang, Y. M.; Belcher, A. M. Virus enabled synthesis and assembly of nanowires for lithium ion battery electrodes. *Science* **2006**, *312*, 885–888.
- [12] Park, M. H.; Kim, M. G.; Joo, J.; Kim, K.; Ki, J.; Ahn, S.; Cui, Y.; Cho, J. Silicon nanotube battery anode. *Nano Lett.* **2009**, *9*, 3844–3847.
- [13] Chan, C. K.; Peng, H.; Lio, G.; McIlwrath, K.; Zhang, X. F.; Huggins, R. A.; Cui, Y. High-performance lithium battery anodes using silicon nanowires. *Nat. Nanotechnol.* **2008**, *3*, 31–35.
- [14] Madasinski, A.; Dixon, P.; Hertzberg, B.; Kvit, A.; Ayala, J.; Yushin, G. High-performance lithium-ion anodes using hierarchical bottom-up approach. *Nat. Mater.* **2010**, *9*, 353–358.
- [15] Li, F.; Xu, J.; Yu, X.; Chen, L.; Zhu, J.; Yang, Z.; Xin, X. One-step solid-state reaction synthesis and gas sensing property of tin oxide nanoparticles. *Sens. Actuators B* **2002**, *81*, 165–169.
- [16] Wang, C. C.; Ying, J. Y. Sol-gel synthesis and hydrothermal processing of anatase and rutile titania nanocrystals. *Chem. Mater.* **1999**, *11*, 3113–3120.
- [17] Wei, B.; Subramanian, V.; Zhu, H. Nanostructured MnO_2 : Hydrothermal synthesis and electrochemical properties as a supercapacitor electrode material. *J. Power Sources* **2006**, *159*, 361–364.
- [18] Sharma, Y.; Sharma, N.; Subba Rao, G. V.; Chowdary, B. V. R. Nanophase ZnCo_2O_4 as a high performance anode material for Li-ion batteries. *Adv. Funct. Mater.* **2007**, *17*, 2855–2861.
- [19] Alcàntara, R.; Jaraba, M.; Lavela, P.; Tirado, L. NiCo_2O_4 spinel: First report on a transition metal oxide for the negative electrode of sodium-ion batteries. *Chem. Mater.* **2002**, *14*, 2847–2848.
- [20] Yang, Y.; Zhao, Y.; Xiao, L.; Zhang, L. Nanocrystalline ZnMn_2O_4 as a novel lithium-storage material. *Electrochim. Commun.* **2008**, *10*, 1117–1120.
- [21] Xiao, L.; Yang, Y.; Yin, J.; Li, Q.; Zhang, Li. Low temperature synthesis of flower-like ZnMn_2O_4 superstructures with enhanced electrochemical lithium storage. *J. Power Sources* **2009**, *194*, 1089–1093.
- [22] Lee, H. W.; Muralidharan, P.; Ruffo, R.; Mari, C. M.; Cui, Y.; Kim, D. K. Ultrathin spinel LiMn_2O_4 nanowires as high power cathode materials for Li-ion batteries. *Nano Lett.* **2010**, *10*, 3852–3856.